

Flow Induced Oscillations of Marine Risers with Wake Interference

Filip Van den Abeele^{*1} and John Vande Voorde¹

¹OCAS N.V., J.F. Kennedylaan 3, BE-9060 Zelzate

*Corresponding author: filip.vandenabeele@arcelormittal.com

Abstract: With offshore oil and gas exploration and production moving into ever deeper waters, the suspended length of marine risers (transporting hydrocarbons from the seabed to the surface) can easily exceed 3000 meters. One of the major design requirements for risers in (ultra)deep water is to limit the fatigue damage caused by vortex induced vibrations (VIV).

Even moderate currents can induce vortex shedding, at a rate determined by the flow velocity. Each time a vortex sheds, a force is generated in both the in-line and cross-flow direction, causing an oscillatory multi-mode vibration. Moreover, both the magnitude and the direction of the current change with water depth, giving rise to higher harmonics in the VIV response of marine risers. Vortex induced vibration can give rise to cyclic stresses that might cause fatigue failure. The huge financial loss associated with riser failure is an important incentive to develop more enhanced numerical tools to predict the VIV response of offshore structures.

In this paper, the computational fluid dynamics capabilities of COMSOL Multiphysics are applied to study the behaviour of adjacent risers. For risers in tandem arrangements, the safe distance required to avoid contact between adjacent risers is calculated.

When the cylinders are in close proximity, the formation of both vortex streets is affected by the interference. For sufficiently large spacing between the cylinders, only the formation of the vortex street behind the rear cylinder is affected. The wake interference models are then applied to study multiple risers with different diameters. In the end, the legs of an offshore platform are simulated as well.

Keywords: computational fluid dynamics, fluid structure interaction, vortex induced vibrations, marine risers, wake interference

1. Introduction

The increasing demand for oil and gas, currently estimated at 135 million barrels of oil equivalent per day [01], keeps pushing the boundaries of offshore engineering into ever deeper waters. For instance, Shell's Perdido platform is operating in the Gulf of Mexico in a water depth of 3000 meters. Like shown on Figure 1, more than 120 km of oil pipelines and 160 km of gas pipelines are used to connect this ultra deep water spar platform with the subsea completions [02].

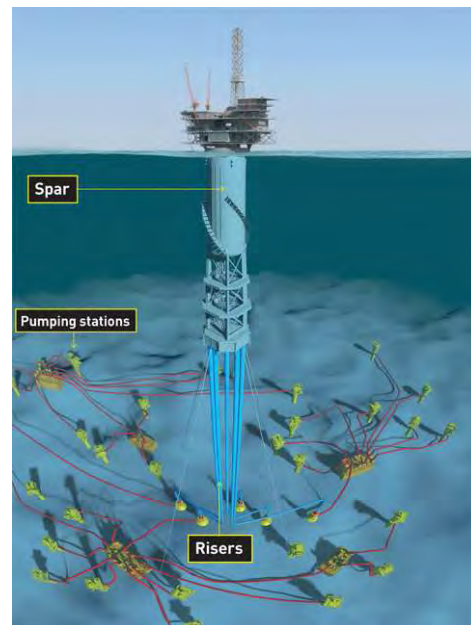


Figure 1. Shell's Perdido platform [02]

For such deepwater developments, the suspended length of the marine risers adds up to several kilometres. A riser is a conductor pipe which connects the wellhead at the seabed to the floating platform or vessel. The riser must sustain production and drilling operations (e.g. carry drilling muds and tools) while withstanding motions induced by currents and waves.

Wall thickness design for marine risers is based on Barlow's formula [03]

$$\sigma_h = \frac{p_i D}{2t} \leq k \sigma_y \quad (01)$$

which states that the hoop stress σ_h , expressed as a function of internal pressure p_i , diameter D and wall thickness t , is limited by the specified minimum yield stress σ_y of the material and a safety factor $k = 0.6$ for hazardous service. Additional design guidelines are applied to account for corrosion allowance and continuity of the internal diameter.

Barlow's formula (01) shows that a smaller diameter riser can convey hydrocarbons at a higher internal pressure. Hence, multiple small diameter risers are typically preferred over one single large diameter riser. During the design of floating production platforms in deepwater, it has been recognized [04] that there is a risk of interference between adjacent production or export risers, or possibly between other combinations of tendons, drilling risers and production risers.

In this paper, interference between multiple marine risers is studied. First, a short review of vortex induced vibrations (VIV) is given. Then, computational fluid dynamics (CFD) is applied to study wake interference of adjacent marine risers in tandem arrangement. The COMSOL model is then extended to simulate multiple risers in tandem and staggered arrangements. In the end, the application of the model to predict the stability of offshore platform legs is briefly addressed.

2. Vortex Induced Vibrations

Subsea structures are subjected to current and wave loading, which induce lift, drag and inertia forces. These forces are described by the Morrison's equations [05]

$$F_D = \frac{1}{2} C_D \rho_w D U |U| \quad (02)$$

$$F_L = \frac{1}{2} C_L \rho_w D U^2 \quad (03)$$

$$F_I = C_I \rho_w \frac{\pi D^2}{4} a \quad (04)$$

where C_L , C_D and C_I are the hydrodynamic coefficients, ρ_w is the density of sea water, U is the flow velocity and a the wave-induced water particle acceleration. The stability conditions of offshore structures are governed by these equations.

In addition to these forces, a turbulent von Karman vortex street can appear in the wake of a subsea pipeline or marine riser for certain combinations of dimensions and flow velocities. Each time a vortex sheds, a force is generated both in the in-line and cross-flow directions, causing an oscillatory multi-mode vibration. When the vortex shedding frequency is close to the natural frequency of the structure, resonance or 'lock-in' could occur, which may jeopardize the stability of the entire offshore structure. On Figure 2, a von Karman vortex street is shown at the onset of turbulence.

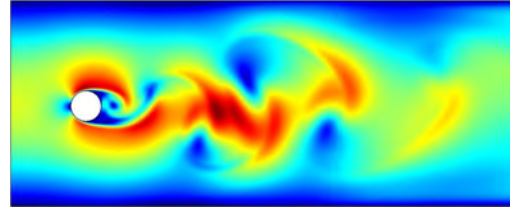


Figure 2. Turbulent Von Karman vortex street

Vortex shedding is governed by the Strouhal number

$$St = \frac{f_s D}{U} \quad (05)$$

where f_s is the vortex shedding frequency, D is the diameter of the riser and U is the flow velocity. The Strouhal number is a function of the Reynolds number

$$Re = \frac{U D}{\nu} \quad (06)$$

which expresses the ratio of inertia forces to viscous forces, with the kinematic viscosity

$$\nu = \frac{\mu}{\rho_w} \quad (07)$$

as the ratio of the dynamic viscosity μ with the density ρ_w .

A slender structure like a marine riser will start to oscillate in-line with the flow when the vortex shedding frequency

$$f_s \approx \frac{1}{3} \frac{\omega_0}{2\pi} \quad (08)$$

with ω_0 the lowest natural frequency of the riser, given by

$$\omega_0 = \frac{C}{L^2} \sqrt{\frac{EI}{m_e}} \quad (09)$$

with C the end boundary coefficient, E the Young's modulus of the material and

$$I = \frac{\pi}{64} (D_o^4 - D_i^4) \quad (10)$$

the moment of inertia, where

$$D_i = D_o - 2t \quad (11)$$

is the inner diameter of the riser. The effective mass m_e includes mass of the steel structure

$$\begin{aligned} m &= \rho_{st} \frac{\pi}{4} (D_o^2 - D_i^2) \\ &= \rho_{st} \pi (D_o - t)t \end{aligned} \quad (12)$$

the internal fluid mass

$$m_i = \rho_i \frac{\pi D_i^2}{4} \quad (13)$$

and the added mass

$$m_a = C_a \rho_w \frac{\pi D_o^2}{4} \quad (14)$$

where the added mass coefficient $C_a = 1$ for vertical pipes and risers. Figure 3 shows the evolution of the drag (02) and lift (03) forces when the von Karman vortex street is fully developed. Note that the average lift force is zero, while the average drag force is a measure for the resistance against fluid flow.

Due to the alternating vortex wake, the oscillations in lift force $F_L(t)$ occur at the vortex shedding frequency f_s , and oscillations in drag force $F_D(t)$ occur at twice this frequency. These oscillations can give rise to an '8-shaped' motion of the marine riser, which is detrimental to its fatigue resistance.

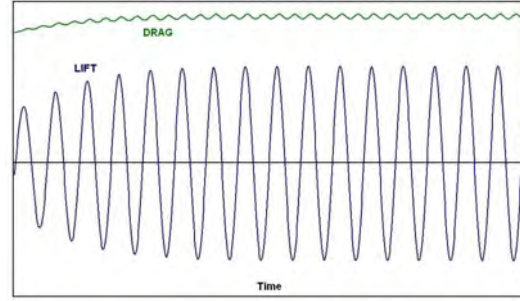


Figure 3. Fluctuating lift and drag forces

A comprehensive review on vortex induced is given in [06]. The implications of VIV on the design of marine risers are addressed in [07-09]. Details on fluid-structure interaction to predict flow induced oscillations in marine risers are given in [10-11], while the use of COMSOL multiphysics is highlighted in [12-13]. In this paper, these modelling techniques are applied to study proximity effects of adjacent marine risers exhibiting wake interference.

3. Flow Patterns for Two Tandem Risers

A careful review of flow interference between two circular cylinders in various arrangements has been presented by Zdravkovich [14], including an extensive list of references on this subject. Different studies for the tandem arrangement of two adjacent risers [15-18] have shown that the changes in drag, lift and vortex shedding are not continuous. Instead, an abrupt change for all flow characteristics is observed at a critical spacing between the risers.

In this section, COMSOL Multiphysics is applied to predict the optimal spacing between two adjacent risers in order to reduce excessive drag and avoid contact or collision. The simulation setup is shown on Figure 4.

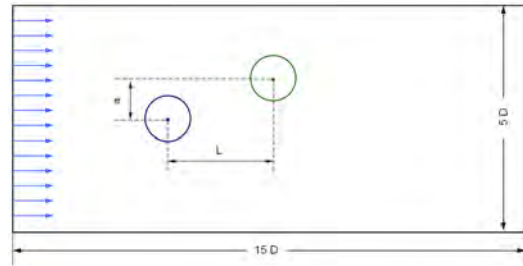


Figure 4. Simulation setup for tandem risers

The fluid flow velocity can be expressed as

$$u(t) = U_1 + U_2 \cos(\omega t) \quad (15)$$

to account for both steady tidal currents and oscillatory flow induced by waves. For a more detailed description of the current profiles for deepwater risers design, the reader is referred to [19]. The horizontal spacing between the risers is shown as L , while $e \neq 0$ allows simulating risers in staggered arrangements as well. The simulated grid is 15D by 5D.

The Computational Fluid Dynamics solver of COMSOL Multiphysics uses a generalized version of the Navier-Stokes equations solving for the velocity field $\vec{u} = (u, v)$ and the pressure p :

$$\begin{aligned} & -\vec{\nabla} \cdot \left[-p \vec{I} + \eta (\nabla \vec{u} + (\nabla \vec{u})^T) \right] \\ & + \rho_w \frac{\partial \vec{u}}{\partial t} + \rho_w (\vec{u} \cdot \vec{\nabla}) \vec{u} = \vec{F} \end{aligned} \quad (16)$$

whilst

$$-\vec{\nabla} \cdot \vec{u} = 0 \quad (17)$$

On Figure 5, the flow pattern is shown for two adjacent risers with $L/D = 2$.

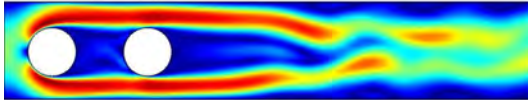


Figure 5. Flow patterns for tandem risers and $L/D = 2$

It has been shown experimentally [15-18] that there is strong interference between two cylinders in tandem arrangement for spacing ratios with $L/D < 3.5$. At a spacing $L/D \approx 3.5$, a sudden change of the flow pattern in the gap between the adjacent risers is observed. The parametric finite element model, shown on Figure 4, enables an easy and straightforward means to evaluate the influence of riser spacing. On Figure 6, flow patterns for different spacings L/D are shown, indeed endorsing the experimental observations for Allen [04], King [16] and Zdravkovich [17].

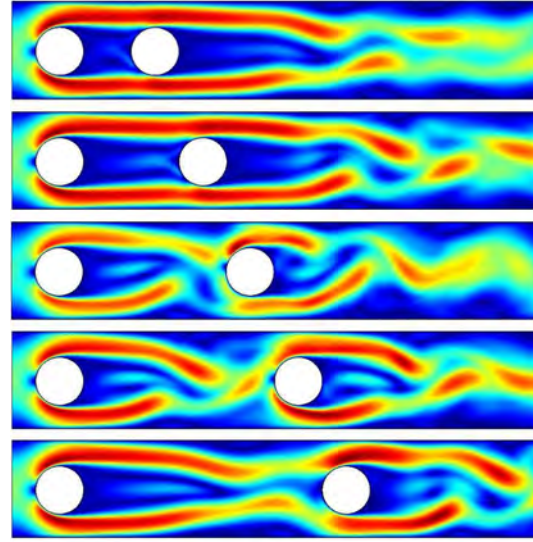


Figure 6. Flow patterns for different riser spacing L/D

Drag coefficient data [17-18] shows that the upstream cylinder takes the brunt of the burden, and that the downstream has little or no effect on the upstream one. For different values of spacing L/D , the drag coefficient

$$C_D = \frac{F_D(t)}{\frac{1}{2} \rho \langle U \rangle^2 D} \quad (18)$$

predicted by COMSOL is shown in Figure 7. Clearly, the drag coefficient on the upstream cylinder is not influenced by the downstream one, but a significant change in drag is observed on the downstream cylinder for $L/D > 3.5$.

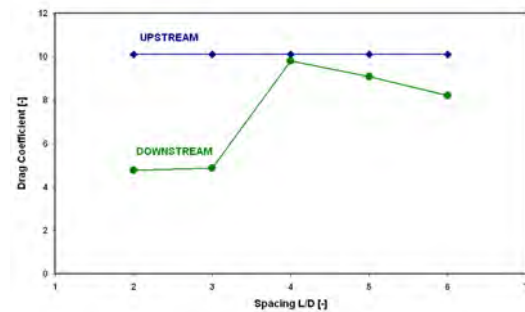


Figure 7. Drag coefficients predicted by COMSOL

More details on proximity effects for risers in tandem arrangements at different flow directions can be found in [17].

4. Multiple Risers in Tandem

Offshore oil and gas production platforms will typically have more than two adjacent risers to convey the hydrocarbons to the surface. On Figure 8, flow patterns around multiple risers in tandem arrangements are shown for different spacings ($L/D = 2$ and $L/D = 3$).

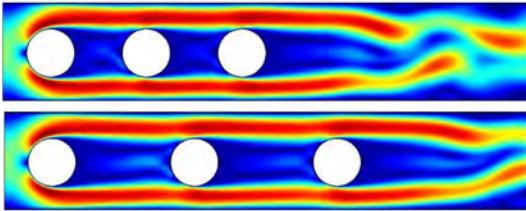


Figure 8. Multiple risers in tandem arrangement

The drag coefficient data of Figure 9 shows that the drag for the upstream cylinder is constant, and that the middle and downstream cylinder drag coefficients are smaller. In other words, there is a strong mutual interference between the middle and downstream cylinder, but only a partial interaction between the upstream and downstream cylinders.

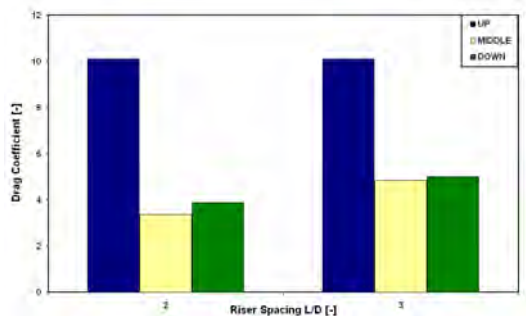


Figure 9. Drag coefficients for multiple risers

The numerical simulations are in close agreement with [20], where an experimental investigation of the effects of spacing on the drag coefficient for a group of three cylinders is reported. The unsteady wake behind a group of parallel cylinders has also been studied in [21].

Figure 10 proves that the diameter of the different risers can have a significant influence on their wake interference. For instance, when production and drilling risers are interacting, or when production risers are shielded by tendons, different flow patterns may arise.

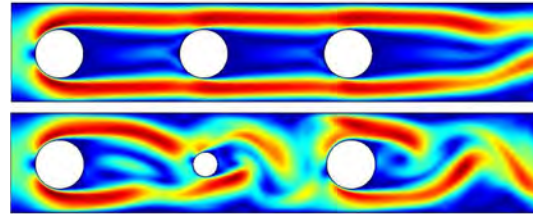


Figure 10. Multiple risers with different diameters

When the middle cylinder is replaced by a smaller one (with diameter $d = D/2$), a totally different flow pattern emerges. As a result, the drag coefficient on the downstream cylinder nearly doubles, while the middle cylinder is shielded by the large diameter cylinders. The fluctuating drag on the (small) middle cylinder and the downstream one are shown on Figure 11.

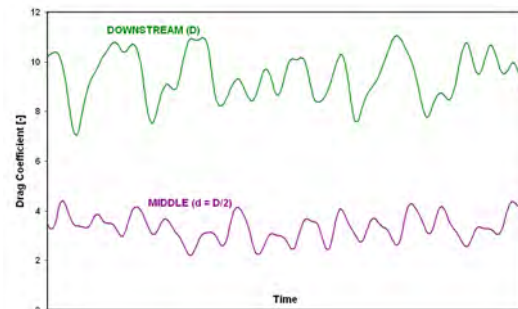


Figure 11. Drag coefficients for different diameters

5. Risers in Staggered Arrangements

Circular cylinders in staggered arrangement have been studied in [17] and [22]. The results show that the upstream and downstream cylinders may be subjected to significantly different lift and drag forces. Depending on their relative positions, the cylinders may experience negligible or strong lift, and reduced or enhanced drag forces.

6. Application to Platform Legs

The wake interference models, presented in this paper, could be applied to simulate flow patterns around offshore platform legs as well. Figure 12 shows a turbulent flow pattern around the four legs of an offshore platform, indicating that they act as independent oscillators.

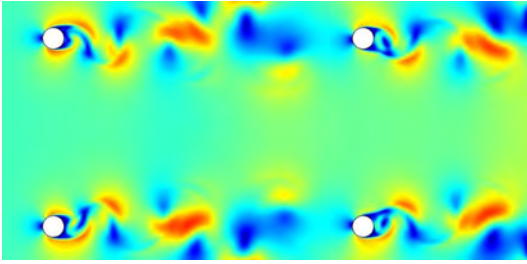


Figure 12. Turbulent flow around offshore platform

Sarpkaya [05] provides some guidelines when applying flow interference models to simulate platform legs:

- The length of an ideal, finite vortex street on either side of a cylinder cannot exceed about half the wave height or the amplitude of flow oscillations. Hence, one may assume that the interference will be negligible if the spacing between the platform legs is greater than half the wave length.
- In a wake comprised of turbulent vortices, the vortex strength decays rapidly. In a distance of some ten diameters, the vortex strength decreases with more than 90%
- The velocity is not constant, but varies from zero to its maximum value during a half cycle. As a result, the use of half wave height as a criterion in determining the interference free spacing may be too conservative.

In Figure 13, the drag coefficients are shown for an upstream and downstream leg of the platform shown in Figure 12. This picture indeed indicates that the platform legs act as independent oscillators.

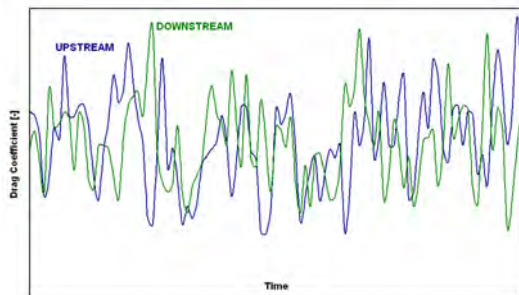


Figure 13. Drag coefficient for platform legs

7. Conclusions

In this paper, the CFD capabilities of COMSOL Multiphysics were applied to investigate proximity effects for adjacent marine risers exhibiting wake interference. The main conclusions read:

- For two risers in tandem arrangement, there is a sudden change in flow characteristics for a critical spacing $L/D \approx 3.5$.
- The upstream riser takes most of the burden. The drag coefficient of the downstream riser(s) is typically lower, depending on the spacing and the Reynolds number.
- The wake interference models, presented here, can successfully be applied to multiple risers with different diameters.
- A difference in diameter can have a significant effect on the flow pattern and, subsequently, the drag experienced by the downstream cylinders.
- Wake interference models can be applied to simulate platform legs as well. Normally, the offshore platform dimensions are such that the legs will act as independent oscillators.

8. References

01. International Energy Agency, *Key World Energy Statistics*, 82 pp. (2010)
02. G.T. Ju, H.S. Littell, T.B. Cook, M. Dupre, K.M. Clausing, E. Shumilak and W.W. Schoppa, Perdido Development: Subsea and Flowline Systems, *Proceedings of the Offshore Technology Conference*, OTC-20882 (2010)
03. M. Mohitpour, H. Golshan and A. Murray, Pipeline Design and Construction – A Practical Approach, Third Edition, *ASME Press* (2007)
04. D.W. Allen, D.L. Henning and L. Lee, Riser Interference Tests on Flexible Tubulars at Prototype Reynolds Numbers, *Proceedings of the Offshore Technology Conference*, OTC-17290 (2005)

05. T. Sarpkaya and M. Isaacson, Mechanics of Wave Forces on Offshore Structures, *Van Nostrand Reinhold*, New York, 651 pp. (1981)
06. R.D. Gabbai, H. Benaroya, An Overview of Modelling and Experiments of Vortex Induced Vibrations for Circular Cylinders, *Journal of Sound and Vibration* vol. 282, pp. 575-616 (2005)
07. E.I. Ofougbu, Review of Vortex Induced Vibrations in Marine Risers, *M.Sc. Thesis*, Cranfield University, School of Applied Science, Offshore and Ocean Technology (2008)
08. A. Ashiru, Assessment of Vortex Induced Vibration Response in Higher Harmonics Mode, *M.Sc. Thesis*, Cranfield University, School of Applied Sciences, Offshore and Ocean Technology (2007)
09. J.M. Shanks, Static and Dynamic Analysis of Marine Pipelines and Risers, *PhD Thesis*, Cranfield Institute of Technology, College of Aeronautics (1985)
10. M. Dixon and D. Charlesworth, Application of CFD for Vortex Induced Vibration Analysis of Marine Risers in Projects, *Proceedings of the Offshore Technology Conference*, OTC-18348 (2006)
11. K. Huang, H.C. Chen and C.R. Chen, Deepwater Riser VIV Assessment by Using a Time Domain Simulation Approach, *Proceedings of the Offshore Technology Conference*, OTC-18769 (2007)
12. F. Van den Abeele, J. Vande Voorde and P. Goes, Fluid Structure Interaction to Predict Fatigue Properties of Subsea Pipelines Subjected to Vortex Induced Vibrations, *Proceedings of the 5th Pipeline Technology Conference*, Ostend, Belgium (2009)
13. F. Van den Abeele, J. Vande Voorde and P. Goes, Numerical Modelling of Vortex Induced Vibrations in Submarine Pipelines, *Proceedings of the 3rd COMSOL Users' Conference*, Hannover, Germany (2008)
14. M.M. Zdravkovich, Review of Flow Interference between Two Circular Cylinders in Various Arrangements, *Journal of Fluids Engineering*, vol. 99(4), pp. 618-633 (1977)
15. D.W. Allen and D.L. Henning, Vortex Induced Vibration Current Tank Tests of Two Equal Diameter Cylinders in Tandem, *Journal of Fluids and Structures*, vol. 17, pp. 767-781 (2003)
16. R. King, Wake Interaction Experiments with Two Flexible Circular Cylinders in Flowing Water, *Journal of Sound and Vibration*, vol. 45(2), pp. 559-583 (1976)
17. M.M. Zdravkovich, Flow Induced Oscillations of Two Interfering Circular Cylinders, *Journal of Sound and Vibration*, vol. 101(4), pp. 511-521 (1985)
18. H. Zhang and W.H. Melbourne, Interference between Two Cylinders in Tandem in Turbulent Flow, *Journal of Wind Engineering and Industrial Aerodynamics*, vol. 41-44, pp. 589-600 (1992)
19. A.J. Adams, W.S. Atkins and J.L. Thorogood, On the Choice of Current Profiles for Deepwater Riser Design, *Proceedings of the SPE Annual Technical Conference*, Society for Petroleum Engineers, SPE-49262 (1998).
20. C. Dalton and J.M. Szabo, Drag on a Group of Cylinders, *ASME Paper 76-Pet-42* (1976)
21. A.S. Mujumdar and W.J.M. Douglas, The Unsteady Wake Behind a Group of Three Parallel Cylinders, *ASME Paper 70-Pet-8* (1970)
22. S. Mittal and V. Kumar, Flow Induced Oscillations of Two Cylinders in Tandem and Staggered Arrangements, *Journal of Fluids and Structures*, vol. 15, pp. 717-736 (2001)